High Order Dynamic Model and Control Strategy of Automotive Powertrain System with Electro-hydraulic Driven Dry-clutch

Dr. Mario PISATURO[1], Prof. Dr. Adolfo SENATORE[1,*]

[1] Department of Industrial Eng., University of Salerno, {mpisaturo,a.senatore}@unisa.it

[*] *corresponding author*

Abstract: *In Automated Manual Transmissions (AMTs) based on electro-actuated dry-clutch design the frictional material properties, the sensors accuracy, the response of the throwout bearing actuator, and the control strategies to drive the engagement operation are mutual interdependent and only an optimized mechatronic design could lead to an effective target from several points of view: passengers' comfort, fuel economy, system reliability, performance, driving feeling, etc.*

In such transmissions, the quality of the vehicle propulsion as perceived by driver and passengers is largely dependent on either the quality of the control strategies and the fast dynamics of the clutch subsystems. Furthermore, sensitivity analyses on control schemes for this type of transmissions have shown that uncertainties on the prediction of the actual torque transmitted by the clutch can severely affect the engagement performance.

In this paper a high order dynamic model of the powertrain system which includes the electro-hydraulic actuator dynamics has been analysed to design a feedback controller based on multiple Model Predictive Controller (MPC). Simulations of start-up manoeuvres prove the effectiveness of the proposed control strategy and encourage the development of real-time routines for the testing on transmission control unit.

Keywords*: electro-hydraulic actuator, dry-clutch control, mechatronic transmission, simulation*

1. Introduction

An Automated Manual Transmission (AMT) is directly derived from a manual one through the integration of actuators. In this way, development and production costs are generally lower than other automatic transmissions, while the reliability and durability are at highest level. For high class sport cars, vehicle dynamic performances and driving quality can be strongly improved with respect to automatic transmissions [1,2].

In AMTs the clutch engagement during gearshift is managed by an actuator driven by the Transmission Control Unit (TCU). Consequently, high importance is assumed by the actuator positioning accuracy along with the reliability of the control algorithm implemented in the TCU. Several models of control strategies for dry clutches in AMTs have been proposed in the literature, e.g., classical controller [2], decoupling control [3], optimal control [4,5], predictive control [6,7], and robust control [8,9]. However, as explained in [10] effective AMTs controllers are difficult to be designed without having a physical model to predict the actual frictional torque transmitted by the clutch.

On the other hand, the improvement of the engagement smoothness has driven the vehicle designers to deepen about vibrations that arise during the clutch operations to prevent poor ride quality, discomfort and noise. The control systems in modern automated manual transmission systems couldn't provide good improvement of vehicle longitudinal dynamics during gearshifts without a deep knowledge of the driveline stiffness and damping parameters, along with the frictional conjunction between its main subparts. To this end, more phenomena about vibrations and actuation noises in clutch and gearbox (e.g., judder, shuffle, eek, whoop, clunk, scratch, etc.) have been identified and analyzed [11-17].

In this paper a high order dynamic model of the powertrain system which includes the electro-hydraulic actuator dynamics has been analyzed to design a feedback controller based on multiple Model Predictive Controller (MPC) [6,18]. The MPC is developed to comply with constraints both on the inputs and the outputs. The controller aims at ensuring a comfortable lock-up by avoiding

the engine stall as well even with reduced engagement time. One of the main factors which have led to use the MPC approach could be found in its ability to explicitly handle the constraints. This means that the controller allows for input constraints, like for example actuator saturation constraints, and it never generates input signal that attempt to violate them. Thus, with predictive control the wind-up problem does not arise [19]. Furthermore, with the rapid development of computing, MPC becomes more and more attractive feedback strategy in fast dynamics systems [20].

Simulations of start-up manoeuvres prove the effectiveness of the proposed control strategy and encourage the development of real-time routines for the testing on transmission control unit.

2. Driveline Model

This section describes a model for simulating the driveline dynamic behaviour; the Fig. 1 shows the driveline main subparts on the left side and its model, on the right. The subscripts e, f, c, g, w are referred to engine, flywheel, clutch disc, (primary shaft of) gearbox, and wheels, respectively. A dynamic model of the driveline can be obtained by applying the d'Alembert equilibrium at the nodes of the driveline scheme, where indicates the *T* torques, *J* the inertias and θ the angles.

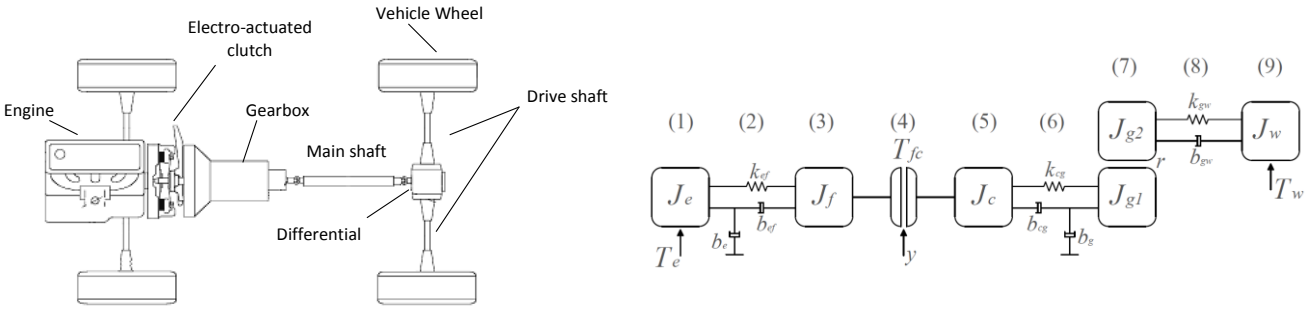

(a) (b)

Fig. 1. (a) car driveline and (b) 5 degree-of-freedom driveline model

The equations which model the driveline are:

$$J_e\dot{\omega}_e = T_e(\omega_e) - b_e\omega_e - T_{ef}(\vartheta_{ef}, \omega_{ef}) \tag{1}$$

$$J_f\dot{\omega}_f = T_{ef}(\vartheta_{ef}, \omega_{ef}) - T_{fc}(x_{to}) \tag{2}$$

$$J_c\dot{\omega}_c = T_{fc}(x_{to}) - T_{cg}(\vartheta_{cg}, \omega_{cg}) \tag{3}$$

$$J_g(r)\dot{\omega}_g = T_{cg}(\vartheta_{cg}, \omega_{cg}) - b_g\omega_g - \frac{1}{r}T_{gw}(\vartheta_{gw}, \omega_{gw}) \tag{4}$$

$$J_w\dot{\omega}_w = T_{gw}(\vartheta_{gw}, \omega_{gw}) - T_w(\omega_w) \tag{5}$$

and the angular speeds are:

$$\dot{\vartheta}_e = \omega_e \tag{6}$$

$$\dot{\vartheta}_{ef} = \omega_{ef} = \omega_e - \omega_f \tag{7}$$

$$\dot{\vartheta}_{cg} = \omega_{cg} = \omega_c - \omega_g \tag{8}$$

$$\dot{\vartheta}_{gw} = \omega_{gw} = \omega_g - \omega_w \tag{9}$$

where T_e is the engine torque (assumed to be a control input of the model), T_{fc} is the torque transmitted by the clutch (the second control input), y is the throwout bearing position, and T_w is the equivalent load torque at the wheels (a measured disturbance). The gear ratio is r (which here includes also the final conversion ratio), and J_c is an equivalent inertia, which includes the masses of the clutch disc, friction pads and the cushion spring.

Furthermore the following equations also hold:

$$J_g(r) = J_{g1} + \frac{J_{g2}}{r^2} \tag{10}$$

$$T_{ef}\left(\vartheta_{ef}, \omega_{ef}\right) = k_{ef}\vartheta_{ef} + b_{ef}\omega_{ef} \tag{11}$$

$$T_{cg}\left(\vartheta_{cg}, \omega_{cg}\right) = k_{cg}\vartheta_{cg} + b_{cg}\omega_{cg} \tag{12}$$

$$T_{gw}\left(\vartheta_{gw}, \omega_{gw}\right) = k_{gw}\vartheta_{gw} + b_{gw}\omega_{gw} \tag{13}$$

$$T_w\left(\omega_w\right) = T_{w0} + \frac{1}{2}\rho_a A c_d R_w^3 \omega_w^2 \tag{14}$$

where k are torsional stiffness coefficients, b viscous damping, T_{w0} a constant load torque, ρ_a the air density, A the front surface vehicle area, c_d the air drag-resistance coefficient, R_w the wheels radius.

These equations represent the driveline system during the slipping phase, whereas, during the engaged phase, the flywheel angular speed ω_f and the clutch angular speed ω_c are the same: thus, the equations (2) and (3) can be summed each other, which yields:

$$\left(J_c + J_f\right)\dot{\omega}_c = T_{ef}\left(\vartheta_{ef}, \omega_{ef}\right) - T_{cg}\left(\vartheta_{cg}, \omega_{cg}\right) \tag{15}$$

The driveline parameters used for the simulation are typical for a mid-size car and can be found in literature. An alternative mathematical representation of the driveline useful for the Model Predictive Control (MPC) approach is the State-Space representation. In the continuous domain the driveline model can be written as follows:

$$\dot{\mathbf{x}}(t) = \left[\mathbf{A}_{sl}d + \mathbf{A}_{eng}\left(1-d\right)\right]\mathbf{x}(t) + \left[\mathbf{B}_{sl}d + \mathbf{B}_{eng}\left(1-d\right)\right]\mathbf{u}(t) \tag{16a}$$

$$\mathbf{y}(t) = \mathbf{C}\mathbf{x}(t) \tag{16b}$$

where the state, input and output vectors are respectively:

$$\mathbf{x} = \left\{\omega_e \quad \vartheta_e \quad \omega_f \quad \vartheta_f \quad \omega_c \quad \vartheta_c \quad \omega_g \quad \vartheta_g \quad \omega_w \quad \vartheta_w\right. \tag{17}$$

$$\mathbf{u} = \left\{T_e \quad T_{fc} \quad T_w\right\}^T \tag{18}$$

$$\mathbf{y} = \left\{\omega_e \quad \omega_c\right\}^T \tag{19}$$

and d is a switching integer equal to *1* when the system is in the slipping phase and *0* otherwise. The subscript *sl* and *eng* indicate the slipping and the engaged system matrices, respectively, and the matrices can be simply deduced from equation (1)-(15).

The MPC has been designed with the discrete time version of the driveline model (16) obtained by using the zero-order hold method with a sampling time of 0.01s. This value is compatible for automotive applications. In fact, as reported in [21] the computational cycle adopted for these applications is set as 5 to 10ms.

3. Actuator Model

In this section a model of the hydraulic actuator system with the usual features of those coupled to AMT systems is introduced. As previously explained, the aim of the actuator is to throwout bearing position and, consequently, the torque transmitted from the engine to the wheels. In this way it is possible to disengage and engage the clutch during the start-up and the gear-shifts manoeuvres.

The actuator is mainly composed by a hydraulic piston connected to a diaphragm spring by the way of a roller bearing ("throwout-bearing") and other springs that keep the clutch closed when no pressure is applied to the piston, Fig. 2. The piston chamber is connected to a servovalve by means of pipeline. The other two-way of the servovalve are connected to a supply circuit and to a discharge circuit, see Fig. 2 for details. The position of the spool valve, which is controlled by an electromagnetic circuit, determines if the hydraulic circuit is in the filling phase or in the dumping phase. The servovalve connects the piston chamber to the discharging circuit in order to disengage the clutch. The springs push the piston back and the oil flows to the tank. Conversely, to engage the clutch the servovalve connects the piston chamber to the supply circuit in this way the piston force overcomes the springs reactions. The servovalve displacement is controlled in current and to keep the clutch at a certain position, an offset current is needed to hold the spool in its neutral point, that corresponds to no oil flowing in the circuit. For currents greater than this offset value, the actuator is connected to the high pressure power supply, while for currents smaller than the offset value, the actuator is connected to the low-pressure circuit [2].

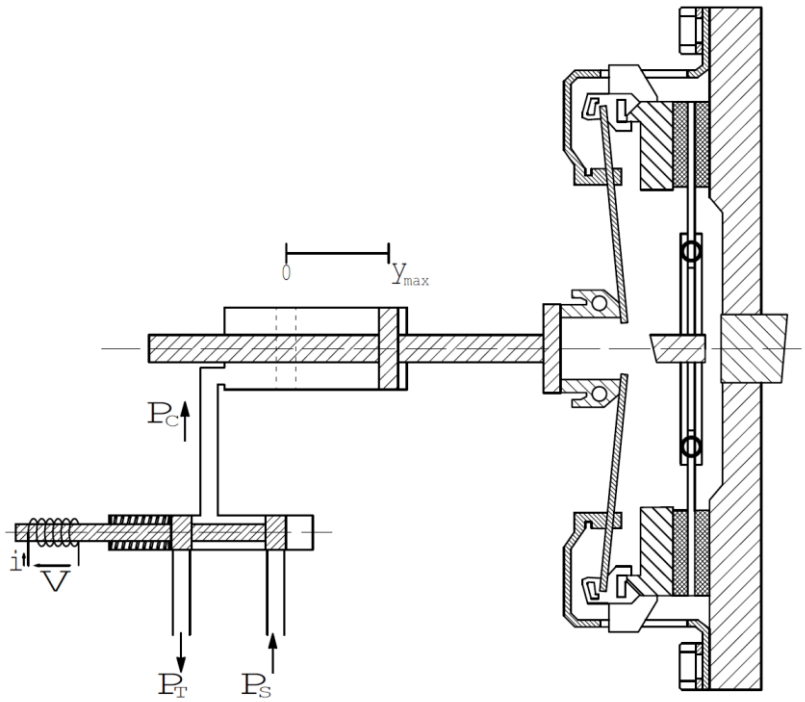

Fig. 2. Actuator scheme and clutch at open position

The clutch actuator is mainly constituted by a mass m_p driven by the springs forces $F_{to}(y)$, friction damping forces and hydraulic forces. The mathematical model which describes the piston dynamics is:

$$m_p\ddot{y} + b_p\dot{y} = A_p P_C - F_{to}(y) \tag{20}$$

$$\dot{P}_C = \frac{\beta}{V_t + A_p y}\left(q(x, P_C) - A_p\dot{y}\right) \tag{21}$$

where y is the piston position, P_c is the pressure in the actuator chamber, m_p is the actuator mass, b_p is the viscous damping, A_p is the actuator cross-sectional area, $F_{to}(y)$ is the diaphragm spring and pre-load force as function of the actuator position (see Fig. 3), V_t is the minimum volume of the chamber at $y=0$, $q(x,P_c)$ is the oil flow given by the eq. (24) and finally β is the bulk modulus of the oil.

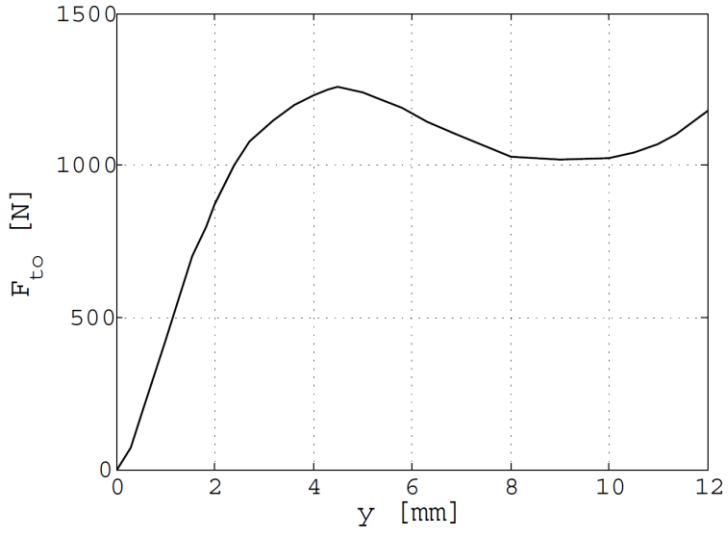

Fig. 3. Diaphragm reaction vs. actuator position

3.1 Servovalve model

A three-way spool flow servovalve with the plunger driven by an electromagnetic actuator has been considered. The servovalve scheme is reported in the Fig. 2 and the mathematical model of the plunger motion is reported below:

$$m_v\ddot{x} + b_v\dot{x} - k_v x = F_M(x, \varphi) + F_B(x, P_C) - F_0 \tag{22}$$

where x is the plunger position, m_v the plunger mass, b_v is the viscous damping, k_v is the stiffness coefficient, F_M is the magnetic force, is the magnetic flux, F_B is the Bernoulli force due to fluid flow through the orifices and F_O is the spring pre-load.

Under usual operating conditions, the magnetic force acting on the servovalve plunger is considered proportional to the valve current. Moreover, by neglecting the Bernoulli force and by designing a high gain current controller, the servovalve can be considered a current-driven actuator [2]. Under this light the relationship between the servovalve current and the plunger position is given by the following equation:

$$x = \frac{-F_0 + k_f i}{k_v} \tag{23}$$

3.2 Hydraulic model

By considering an overlapped valve, i.e. the land width is greater than the port width when the plunger is in the neutral position and consequently no oil flows through the orifices. This means that there is a dead-band in the orifice area vs. plunger position as described in the equation (24). The oil flow through the servovalve can be written according to Bernoulli's equation:

$$q=\begin{cases}\operatorname{sgn}(P_S-P_C)C_d\sqrt{\dfrac{2|P_S-P_C|}{\rho}}f_f(x)\\ 0\\ -\operatorname{sgn}(P_C-P_T)C_d\sqrt{\dfrac{2|P_C-P_T|}{\rho}}f_d(x)\end{cases} \tag{24}$$

where the first case represents the filling phase ($x > x_f$), the second case represents the dead-zone ($x_d \leq x \leq x_f$) and the last case represents the dumping phase ($x < x_d$). C_d is the discharge coefficient, ρ is the oil density, P_s is the supply pressure and P_T is the tank pressure. The functions f_f and f_d describe the relationship between the orifice area vs. plunger position.

$$\begin{cases}f_f(x)=1.3796x^2-1.4197x+0.1335\\ f_d(x)=1.3371x^2-3.0447x+1.4799\end{cases} \tag{25}$$

The actuator parameters used for the simulations are listed in [2].

4. Controller Design

In order to manage the engagement phases two closed loops have been designed, Fig. 4. The outer closed loop manages the driveline dynamics and a multiple Model Predictive Control (MPC) strategy has been implemented. The inner loop supervises the actuator position tracking: a PI controller has been designed by neglecting the sensor dynamics.

The electro-hydraulic actuator dynamics depicted in the section 3 is represented by the block A(z) whereas the "Clutch torque model" introduces the frictional torque based on the elastic properties of diaphragm and cushion springs, the clutch disk geometry and the friction coefficient of the disk facings according to the models and outcomes in [22-24].

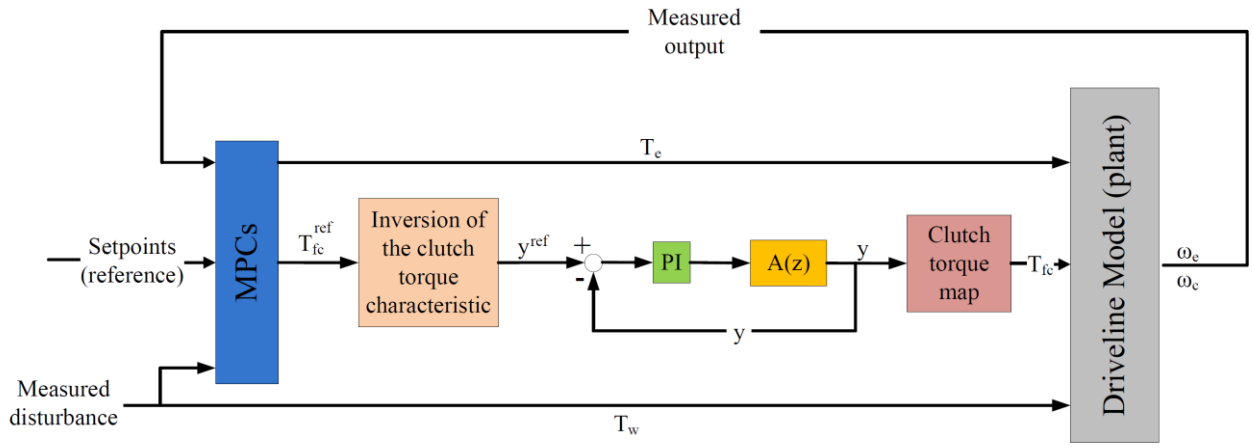

Fig. 4. Block-diagram with MPC-based controller, clutch and driveline models

4.1 Multiple Model Predictive Control

In this section the control approach through MPC theory is explicated. This kind of algorithm provides numerous advantages over the conventional control algorithms. Indeed, it handles multivariable control problem naturally, it can take account of actuator limitations, it allows the system to operate closer to constraints than conventional control, and finally control update rates are relatively low in these applications, so that there is plenty of time for the necessary on-line computations [19].

As explained above, the clutch operates in two different working conditions: the slipping phase and the engaged phase. That is why two different controllers for each phase have been designed. The switching parameter *d* selects the controller by considering the absolute value of the difference between the engine and the clutch angular speed. Particularly, the switching condition is attained when $\omega_{sl}=\omega_e-\omega_c\leq 1$ rad/s.

It is important to emphasize that in no way the two controllers can work simultaneously and so any conflict between them is avoided *a priori*.

The MPC has been designed with the discrete time version of the driveline model (16) obtained by using the zero-order hold method with a sampling time of 0.01 s. As explained above, this value is compatible for automotive applications.

$$\begin{aligned}\mathbf{x}_{k+1} &= \left[\bar{\mathbf{A}}_{sl}d+\bar{\mathbf{A}}_{eng}\left(1-d\right)\right]\mathbf{x}_k+\left[\bar{\mathbf{B}}_{sl}d+\bar{\mathbf{B}}_{eng}\left(1-d\right)\right]\\ \mathbf{y}_k &= \bar{\mathbf{C}}\mathbf{x}_k\end{aligned} \tag{26}$$

The MPC aims at finding the output y_k by tracking the reference trajectory r_k and fulfilling the constraints seen above for any time step $k\geq 0$.

Under the assumption that the estimate of x_k is available at time *k*, the cost function to be optimized is:

$$J_i\left(\Delta u,\varepsilon\right)=\mathbf{u}_i{}^T\mathbf{W}_{u,i}^2\mathbf{u}_i+\Delta\mathbf{u}_i{}^T\mathbf{W}_{\Delta u,i}^2\Delta\mathbf{u}_i+\left[\mathbf{y}_i-\mathbf{r}_i\right]^T\mathbf{W}_{y,i}^2\left[\mathbf{y}_i-\mathbf{r}_i\right]+ \tag{27}$$

where:

$$\mathbf{u}_i=\left[u_i\left(0\right)\quad ...\quad u_i\left(P-1\right)\right]^T \tag{28}$$

is the input vector;

$$\Delta\mathbf{u}_i=\left[\Delta u_i\left(0\right)\quad ...\quad \Delta u_i\left(P-1\right)\right]^T \tag{29}$$

is the input increment vector;

$$\mathbf{y}_i=\left[y_i\left(1\right)\quad ...\quad y_i\left(P\right)\right]^T \tag{30}$$

is the output vector;

$$\mathbf{r}_i=\left[r_i\left(1\right)\quad ...\quad r_i\left(P\right)\right]^T \tag{31}$$

is the reference trajectory vector. $W_{u,i}$, $W_{\Delta u,i}$ and $W_{y,i}$ are, respectively, the input, input increment and output weights matrices (diagonals and squares); the subscript *i=1,2* accounts for the two inputs and two outputs of the "plant". The constraints on *u, Δu, y* are softened by introducing the slack variable $\varepsilon\geq 0$. In (27), the weight ρ_ε on the slack variable ε penalizes the violation of the constraints. As ρ_ε increases with respect to the input and output weights, the controller gives higher priority to the minimization of constraint violations [7].

4.2 Closed-loop actuator control

A classical regulator PI has been designed on the basis of a linearised model of the actuator. In particular, from the non-linear actuator model described by equations (20)-(25) a simplified linear model has been achieved by using a built-in function in MATLAB/SIMULINK©. The local feedback control on the throwout bearing position provides robustness to the closed loop system. The reference bearing position is obtained by inverting the clutch torque signal output of the MPC by a look-up table which represents the inversion of the static clutch torque characteristic as show in the Fig. 4.

The PI parameters $K_P=1.2$ and $K_I=0.5$ have been obtained by trial and error procedure looking for the best trade-off between a fast response and the restriction of the wind up problem.

5. Simulation Results

The simulation results have been obtained by implementing the driveline and the actuator models in the MATLAB/SIMULINK© environment. Two typical vehicle launch manoeuvres has been considered: *slow* and *fast*. The switch between the slipping and the engaged phase is selected by a Stateflow finite state machine. This signal is used both to select the MP controller suitable to manage each phase and to select the part of the driveline model to activate. The switching condition is reached when the value of the slip speed is less than 1 rad/s. Once the clutch is engaged, the throwout bearing position is rapidly increased to its maximum value by the control algorithm. In other words the clutch actuator reaches the rest position.

Figs. 5, 6 and 7 show the results of the controlled AMT in a slow start-up manoeuvre. The behaviours of the engine and angular velocity, set-points and plant outputs, and those of the engine torque and throwout bearing position are depicted. The comparison between the set-points and the plant outputs shows the good performances of the MPC both before that after the clutch engagement. In fact, the clutch speed set-point trajectory is well tracked by the plant output during the engagement phase and together with the engine speed reach in few seconds the regime value. Moreover in the Fig. 6 the effectiveness of the constraints on the engine torque and on its rate have highlighted showing again the good performance of the MPC.

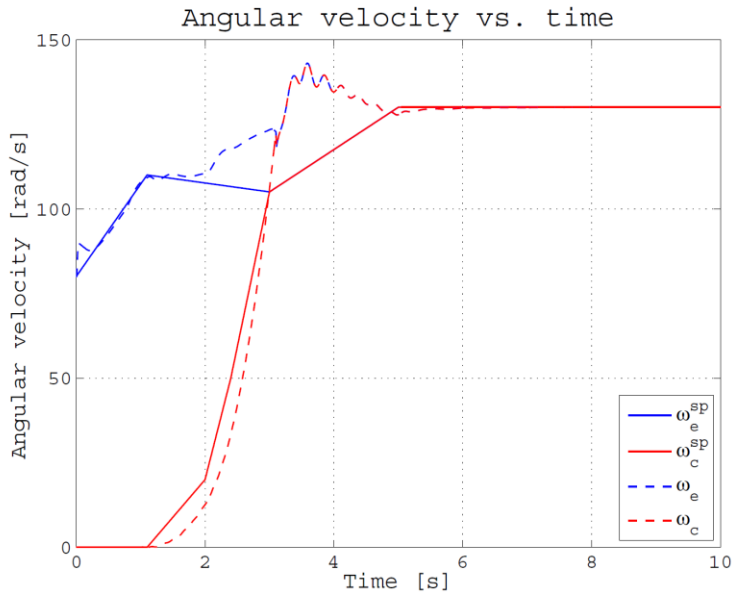

Fig. 5. Slow start-up manoeuvre: angular velocity, set-point trajectory and plant outputs

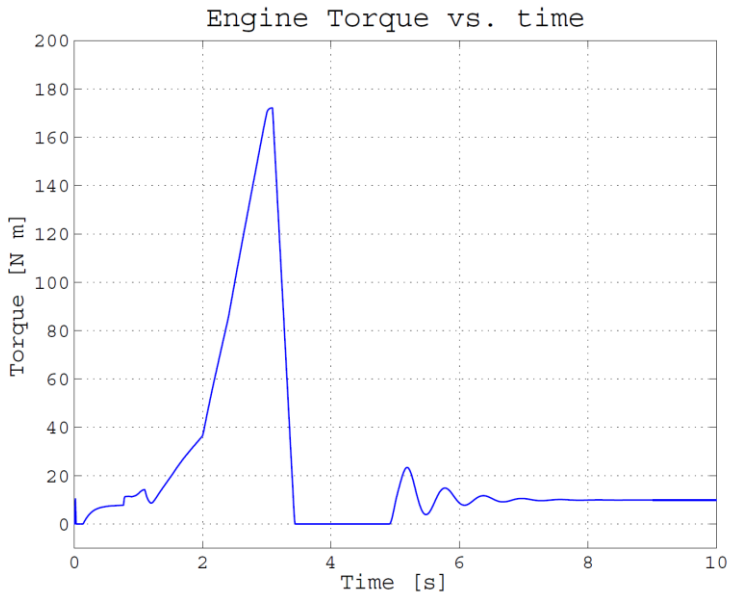

Fig. 6. Slow start-up manoeuvre: engine torque

Finally, in the Fig. 7 the good performance of the PI inner loop on the throwout bearing position is depicted. It is worth noting that with a good choice of the PI parameters KP and KI the wind-up does not arise.

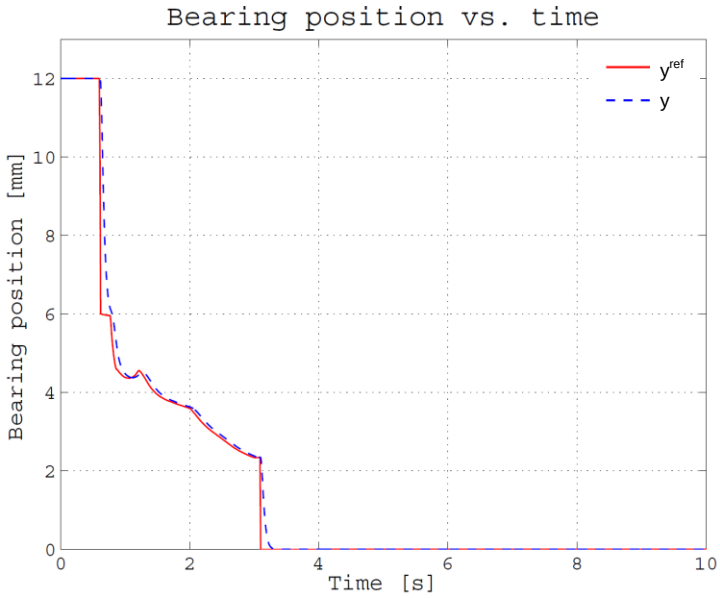

Fig. 7. Slow start-up manoeuvre: throwout bearing position

Figs. 8, 9 and 10 show the results of the controlled AMT in a fast start-up manoeuvre. In this case the comparison between the set-points and the plant outputs shows that for a fast manoeuvre there is an increment of the jerks after that the engagement condition is reached. The Fig. 9 highlights the effectiveness of the constraints on the engine torque and on its rate. Finally, in the Fig. 10 is reported that, also in a fast manoeuvre, the PI controller on the throwout bearing position attains good performances. Indeed, also in this case the wind up does not occur. This means that the throwout bearing position never reaches dangerous and unwanted condition, i.e. excessive stress on the actuator that may be damaged, without the necessity of a saturation on the actuator output highlighting the robustness of the inner closed loop. Figs. 7 and 10 depicts as after that the

engaged condition is attained, the throwout bearing position reaches its rest position. Simulations of the actuator dynamics in open-loop, whose results are not reported here for the sake of briefness, have proven the limits of such industrial cheaper approach concerning the poor tracking of the reference clutch torque.

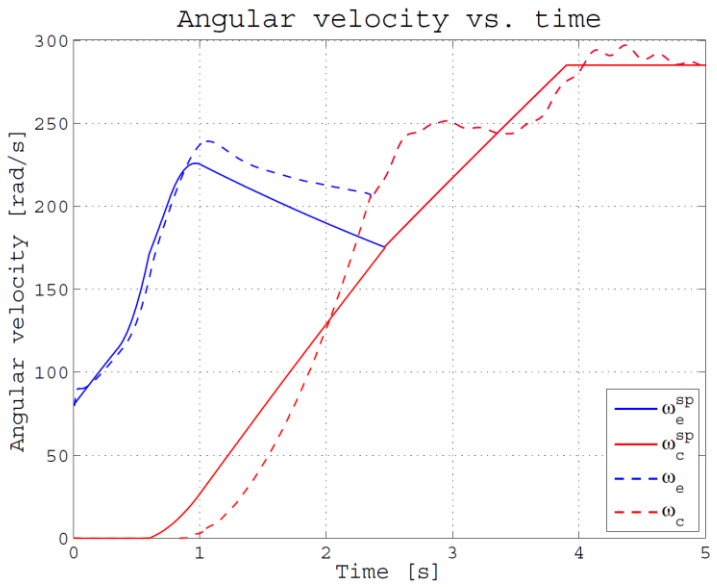

Fig. 8. Fast start-up manoeuvre: angular velocity, set-point trajectory and plant outputs

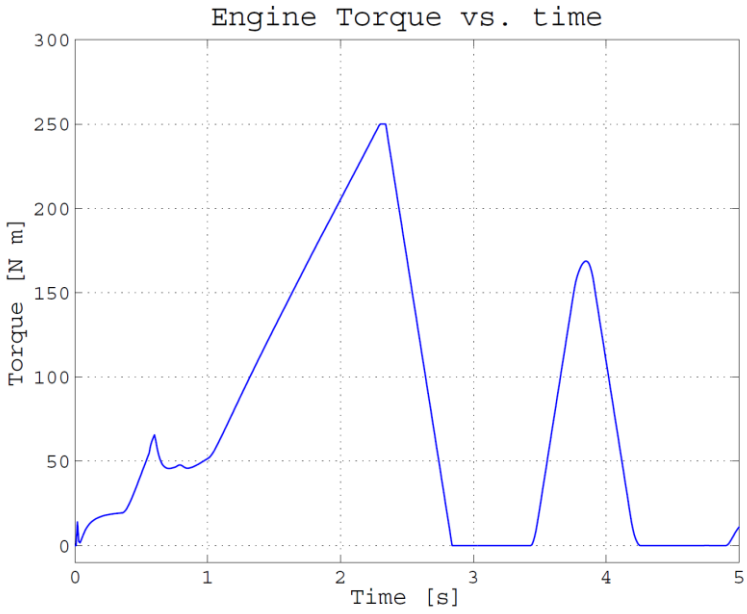

Fig. 9. Fast start-up manoeuvre: engine torque

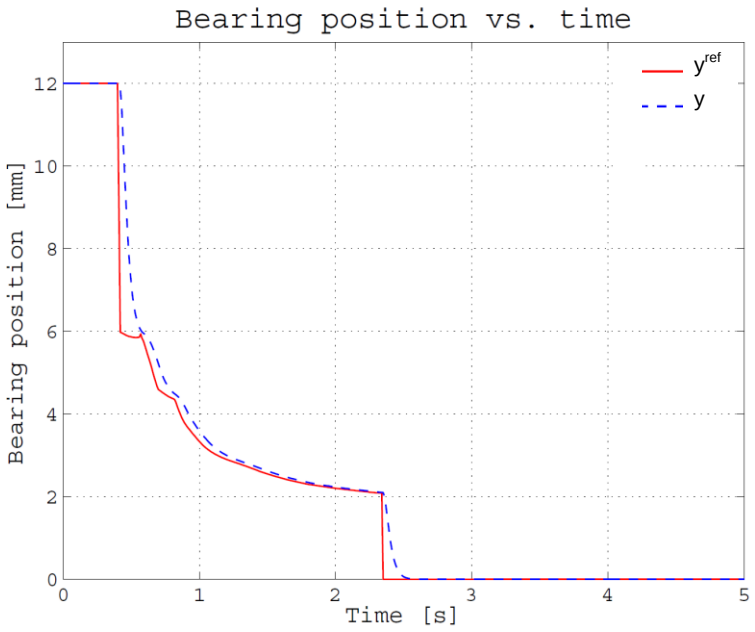

Fig. 10. Fast start-up manoeuvre: throwout bearing position

6. Concluding remarks

In this paper the dynamics of a high-order automotive driveline coupled to dry-clutch system driven by electro-hydraulic actuator has been analyzed to simulate the launch transient manoeuvres of vehicles equipped with robotized (or AMTs) transmission. The frictional torque transmitted from the engine to the vehicle wheels through the dry clutch disks is governed by the constrained multiple model predictive control and its output signals provided to the actuator. Two controllers have been designed: the first one manages the slipping phase whereas the second one manages the engaged phase. Moreover, the clutch actuator dynamics is managed by position-sensing closed loop control by using a PI regulator.

The simulations results have showed the good performances of the MPC especially for a slow start-up manoeuvre. Moreover, the robustness of the PI regulator has been highlighted for both the start-up manoeuvres. Indeed, the good performances exhibited by the PI controller in both the cases is confirmed by the good tracking of the reference signal, by the fast actuator response and by the evidence of the throwout bearing positions which never exceed their limits making the saturation unnecessary. The simulation of the actuator dynamics in open-loop control has showed poor tracking of the reference clutch torque.

Future studies will focus on the role of fast temperature changes due to the huge amount of heat generated at clutch disk facings' interface and the influence of such behaviour on frictional characteristics and actuator response modification.

References

[1] A. Senatore, "Advances in the automotive systems: an overview of Dual-Clutch Transmissions", Recent Patents on Mechanical Engineering, vol. 2, pp. 93–101, 2 2009, ISSN: 2212-7976;
[2] M. Montanari, F. Ronchi, C. Rossi, A. Tilli, and A. Tonielli, "Control and performance evaluation of a clutch servo system with hydraulic actuation", Control Engineering Practice, vol. 12, no. 11, pp. 1369 –1379, 2004, Mechatronic Systems, ISSN: 0967-0661;
[3] L. Glielmo, L. Iannelli, V. Vacca, and F. Vasca, "Gearshift control for Automated Manual Transmissions", IEEE/ASME Transactions on Mechatronics, vol. 11, no. 1, pp. 17–26, 2006, ISSN: 1083-4435;

[4] L. Glielmo, F. Vasca, "Optimal control of dry clutch engagement". Proc. of SAE 2000 World Congr, (2000) March 6-9; Detroit, MI, USA;
[5] P. Dolcini, C. Canudas de Wit, and H. Bechart, "Lurch avoidance strategy and its implementation in AMT vehicles, Mechatronics", vol. 18, pp. 289–300 (2008);
[6] A. Bemporad, F. Borrelli, L. Glielmo, and F. Vasca, "Hybrid control of Dry Clutch engagement", in European Control Conference, Porto, Portugal, 2001, pp. 635–639.
[7] M. Pisaturo, M. Cirrincione, and A. Senatore, "Multiple constrained MPC design for automotive dry clutch engagement", IEEE/ASME Transactions on Mechatronics, vol. 20, no. 1, pp. 469 - 480, 2005, ISSN: 1083-4435;
[8] L. Glielmo, P.O. Gutman, L. Iannelli, and F. Vasca, "Robust smooth engagement of an Automotive Dry Clutch", Proc. 4th IFAC Symp. Mechatronics Syst., September 12 - 14; Heidelberg, Germany, 2006;
[9] G.J.L. Naus, M. Beenakkers, R. Huisman, M.J.G. van de Molengraft, and M. Steinbuch, "Robust control to suppress clutch judder". Proc. of 8th Int. Symp. Adv. Veh. Control, October 6-9; Kobe, Japan, 2008;
[10] F. Vasca, L. Iannelli, A. Senatore, and G. Reale, "Torque transmissibility assessment for automotive Dry-Clutch engagement", Mechatronics, IEEE/ASME Transactions on, vol. 16, no. 3, pp. 564–573, 2011, ISSN: 1083-4435.
[11] A. Senatore, "Vibrations induced by electro-actuated dry clutch in the Eek frequency: excitation in gear-shifting operations", Journal of Mechatronics, Vol. 2, No. 4, 2014, pp. 301-311, ISSN 2326-2885;
[12] H.H. Miyasato, V.G. Segala Simionatto, and M.J. Dias, "Linear powertrain models for NVH phenomena evaluation, Proc. of the XV International Symposium on Dynamic Problems of Mechanics", DINAME 2013, February 17-22; Buzios, Brazil, 2013;
[13] V.G. Segala Simionatto, H.H. Miyasato, and M.J. Dias, "On the influence of the clutch disk's pre-damper parameters on shuffle and clunk phenomena in powertrains", Proc. of the XV International Symposium on Dynamic Problems of Mechanics, DINAME 2013, February 17-22; Buzios, Brazil, 2013;
[14] A. Myklebust, L. Eriksson, "Road slope analysis and filtering for driveline shuffle simulation", Proc. of IFAC Workshop on Engine and Powertrain Control Sim. and Mod., Rueil-Malmaison, France, 2012, pp. 176-183;
[15] D. Centea, H. Rahnejat, M.T. Menday, "Non-linear Multi-Body dynamic analysis for the study of clutch torsional vibrations (Judder)", Applied Mathematical Modelling, vol. 25, pp. 177-192, 2001, ISSN: 0307-904X;
[16] A. Crowther, N. Zhang, D.K. Liu, J. Jeyakumaran, "Analysis and simulation of clutch engagement judder and stick-slip in automotive powertrain systems", Proc. IMechE Part D - J. of Automobile Eng., vol. 218(12), pp. 1427–1446, 2004, ISSN: 0954-4070;
[17] A. Senatore, D. Hochlenert, V. D'Agostino, U. von Wagner, "Driveline dynamics simulation and analysis of the dry clutch friction-induced vibrations in the Eek frequency range", Proc. of ASME-IMECE 2013, November 15-21; San Diego, CA, USA, 2013;
[18] R. Amari, M. Alamir, and P. Tona, "Unified MPC strategy for idle speed control, vehicle start-up and gearing applied to an Automated Manual Transmission", in 17th IFAC World Congress, Seoul, South Korea, 2008;
[19] J. M. Maciejowski, Predictive Control with Constraints, P. Hall, Ed. 2000;
[20] X. Lu, P. Wang, B. Gao, and H. Chen, "Model Predictive Control of AMT clutch during start-up process", in Control and Decision Conference (CCDC), 2011 China, pp. 3204–3209, 2011;
[21] H. Quanan, S. Jian, and L. Lei, "Research on Rapid Testing Platform for TCU of Automated Manual Transmission", in Proceedings of the 2011 Third International Conference on Measuring Technology and Mechatronics Automation - Volume 03, ser. ICMTMA'11, Washington, DC, USA: IEEE Computer Society, 2011, pp. 67–70, ISBN: 978-0-7695-4296-6.
[22] N. Cappetti, M. Pisaturo, and A. Senatore, "Modelling the cushion spring characteristic to enhance the Automated Dry-Clutch performance: the temperature effect", Proc. of the Institution of Mechanical Engineers, Part D: Journal of Automobile Engineering, vol. 226, no. 11, pp. 1472–1482, 2012, ISSN: 0954-4070.
[23] V. D'Agostino, N. Cappetti, M. Pisaturo, and A. Senatore, "Improving the engagement smoothness through multi-variable frictional map in automated dry clutch control", Proc. of the ASME 2012 International Mechanical Engineering Congress and Exposition - November 9-15, Houston, Texas, 2012;
[24] A. Senatore, V. D'Agostino, R. Di Giuda, and V. Petrone, "Experimental investigation and neural network prediction of brakes and clutch material frictional behaviour considering the sliding acceleration influence", Tribology International, Vol. 44, pp. 1199-1207, 2011, ISSN: 0301-679X.